Molecular Crystals and Liquid Crystals
Publication details, including instructions for authors and subscription information:
http://www.tandfonline.com/loi/gmcl16

Phase Transition and Structure Change of Urea Adducts with n-Paraffins and Paraffin-type Compounds

Yozo Chatani [a] , Hideo Anraku [a] & Yukio Taki [a]
[a] Department of Polymer Science, Faculty of Science, Osaka University, Toyonaka, Osaka, 560, Japan
Version of record first published: 28 Mar 2007.

To cite this article: Yozo Chatani , Hideo Anraku & Yukio Taki (1978): Phase Transition and Structure Change of Urea Adducts with n-Paraffins and Paraffin-type Compounds, Molecular Crystals and Liquid Crystals, 48:3-4, 219-231

To link to this article: http://dx.doi.org/10.1080/00268947808083763

Mol. Cryst. Liq. Cryst., 1978, Vol. 48, pp. 219–231

Printed in Holland

Phase Transition and Structure Change of Urea Adducts with *n*-Paraffins and Paraffin-type Compounds

YOZO CHATANI, HIDEO ANRAKU, and YUKIO TAKI

Department of Polymer Science, Faculty of Science, Osaka University, Toyonaka, Osaka 560, Japan

(*Received January 23, 1978; in final form July 26, 1978*)

The phase transition temperatures of urea adducts with many *n*-paraffins and several paraffin-type compounds were measured by differential thermal analysis and the general structure change causing the phase transitions was revealed by X-ray structure analysis. The ordinary hexagonal adducts (high-temperature form) transform commonly into orthorhombic adducts (low-temperature form) except for a few adducts with guest molecules possessing cylindrical shapes. The phase transition can be regarded as an order-disorder transition with respect to the orientation of the guest molecules about the urea channel axis with a cooperative deformation of the urea channels resulting in the orderly orientation of guest molecules below the transition temperatures. The changes in orientation and motion of the guest molecules through the phase transitions are discussed on the basis of X-ray analysis, potential energy and broad-line NMR.

INTRODUCTION

Our preliminary X-ray study[1] of urea adducts with several *n*-paraffins revealed that these adducts transform commonly from the ordinary hexagonal $P6_122$ crystals[2] (denoted as high-temperature form) into orthorhombic $P2_12_12_1$ crystals (low-temperature form) in narrow temperature regions, and the phase transitions were interpreted in terms of an order-disorder transition with respect to the orientation of the guest molecules causing the deformation of honeycomb-like urea channels. The structures of the high- and low-temperature forms are schematically shown in Figure 1 for the sake of subsequent discussions.

Some physico-chemical studies using NMR,[3–6] dielectric relaxation,[7,8] and depolarization thermo-current[9] have served to clarify the characteristics

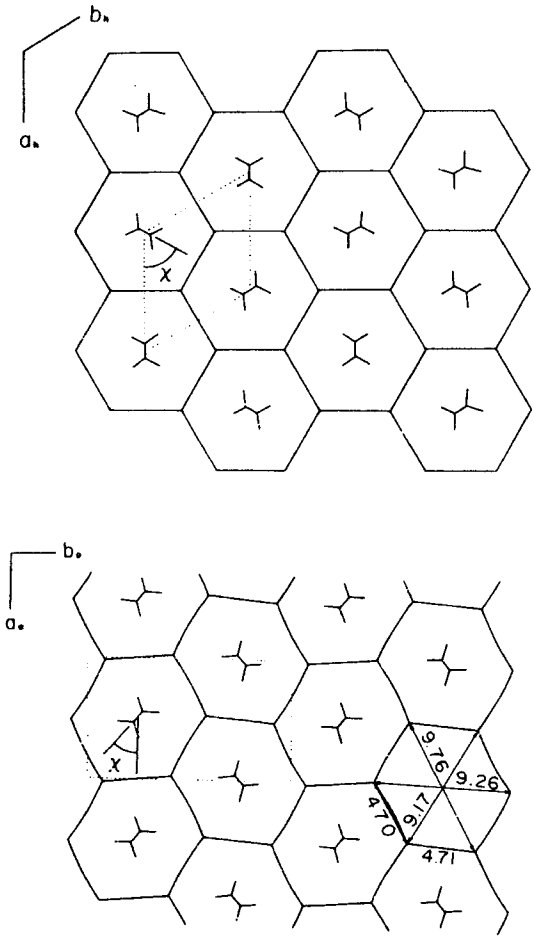

FIGURE 1 Schematic channel structures of the n-$C_{16}H_{34}$-urea adduct viewed along the channel axis. (top) High-temperature form. (bottom) Low-temperature form. Values indicate lengths in A units and χ is the setting angle of guest molecule (see text).

of the rotational motion of the guest molecules. However, these results are not always conclusive, because of a lack of knowledge of the phase transition, of the details of the crystal structure, and especially of the orientation of the guest molecule. Therefore, the present study aims to reveal the structural changes of the order-disorder transitions for the urea adducts with many n-paraffins and paraffin-type compounds by X-ray diffraction, DTA, potential energy and broad-line NMR.

EXPERIMENTAL

The materials examined as guest molecules were *n*-decane $C_{10}H_{22}$, *n*-hexadecane $C_{16}H_{34}$, *n*-octadecane $C_{18}H_{38}$, *n*-icosane $C_{20}H_{42}$, *n*-docosane $C_{22}H_{46}$, *n*-tetracosane $C_{24}H_{50}$, *n*-octacosane $C_{28}H_{58}$, *n*-hexatriacontane $C_{36}H_{74}$, 1,10-dibromodecane $Br(CH_2)_{10}Br$, 1-bromohexadecane $CH_3(CH_2)_{15}Br$, lauric acid $CH_3(CH_2)_{10}COOH$, stearic acid $CH_3(CH_2)_{16}COOH$ and sebacic acid $HOOC(CH_2)_8COOH$. The *n*-paraffins were obtained commercially and described as being of better than 99% purity. All other chemicals were reagent grade and no further purification was made. Urea was recrystallized from methanol solution. Single crystals of the urea adducts with these guests were grown from isopropanol or methanol; in particular, *p*-xylene was added for higher members of the paraffins than *n*-$C_{20}H_{42}$ in order to dissolve them. Another adduct additionally examined was the urea adduct with trans 1,4-polybutadiene $(-CH_2-CH=CH-CH_2-)_n$ which was converted from the 1,3-butadiene-urea adduct on γ-ray irradiation.[10]

Urea-d_4 was obtained by repeated crystallization from D_2O. The $Br(CH_2)_{10}Br$-urea-d_4 and *n*-$C_{20}H_{42}$-urea-d_4 adducts were prepared by recrystallization from CH_3OD.

X-ray diffraction photographs for the single crystals of these adducts were taken with copper Kα radiation at various temperatures from room temperature to 95 K with the aid of a low temperature apparatus designed by the authors. Temperature control was to ± 2.5 K. The cell dimensions of urea adducts were measured with a Weissenberg camera of diameter 90 mm and were calibrated with the cell dimension of aluminum taking into consideration the thermal expansion.[11] DTA measurement was made for powdered samples obtained by crushing slowly the single crystals. The scan was taken at a speed of 3 $Kmin^{-1}$ with the scanning range from room temperature -90 K. Broad-line NMR of the powdered urea-d_4 adducts was measured with a Nihon Denshi JNM-PW60 spectrometer.

TRANSITION TEMPERATURE

Table I shows the transition temperatures of the urea adducts with *n*-paraffins and paraffin-type compounds. These temperatures were estimated from the peak maxima in the DTA curves, because several adducts showed broad peaks spread over 10 degrees. The data of Pemberton and Parsonage[12,13] are also quoted in Table I. Among many adducts examined, the sebacic acid and trans 1,4-polybutadiene adducts did not exhibit exceptionally abnormal heat absorption in the observed temperature range; no distinct

TABLE I

Transition temperatures of urea adducts

Guest	T_i/K
n-$C_{10}H_{22}$	111[a]
n-$C_{11}H_{24}$	122[a]
n-$C_{12}H_{26}$	123[a]
n-$C_{15}H_{32}$	158[a]
n-$C_{16}H_{34}$	152[a]
n-$C_{18}H_{38}$	167
n-$C_{20}H_{42}$	191
n-$C_{22}H_{46}$	178
n-$C_{24}H_{50}$	176
n-$C_{28}H_{58}$	208
n-$C_{36}H_{74}$	218
$Br(CH_2)_{10}Br$	141
$CH_3(CH_2)_{15}Br$	167
$CH_3(CH_2)_{10}COOH$	205
$CH_3(CH_2)_{16}COOH$	239
$HOOC(CH_2)_8COOH$	none
$(-CH_2-CH=CH-CH_2-)_n$	none

[a] Pemberton and Parsonage[12,13]

change in the X-ray diffraction photographs of these adducts took place indeed between room temperature and the lowest temperature of observation, 98 K. All other adducts transformed reversibly from the high-temperature form into the low-temperature form. It is well known that n-paraffin crystals undergo an order-disorder transition with respect to the molecular orientation a few degrees below their melting points. As shown in Figure 2, the transition temperatures of the adducts with even-membered hydrocarbons do not always increase gradually with the number of carbon atoms in the guest molecule differing from the series of even- or odd-membered paraffin crystals.[14] This feature might be caused by the non-integral mole ratios of urea to guests: the increment of paraffin chain length of 2.5 A for two carbon atoms does not fit into the interval of urea molecules, 1.83 A, along the channel axis.

The channel length occupied by a guest molecule was estimated from extra layer lines in the X-ray rotation photograph taken about the channel axis, which appeared by the contribution of guest molecules. The values for stearic acid and lauric acid, 50.13 A and 34.80 A, respectively, are interpreted in terms of the formation of their dimer molecules linked by O—H···O hydrogen bonds.[15] It is interesting that the transition temperatures of the stearic acid and lauric acid adducts satisfy the relation between the transition temperature and the number of carbon atoms for the n-paraffin adducts

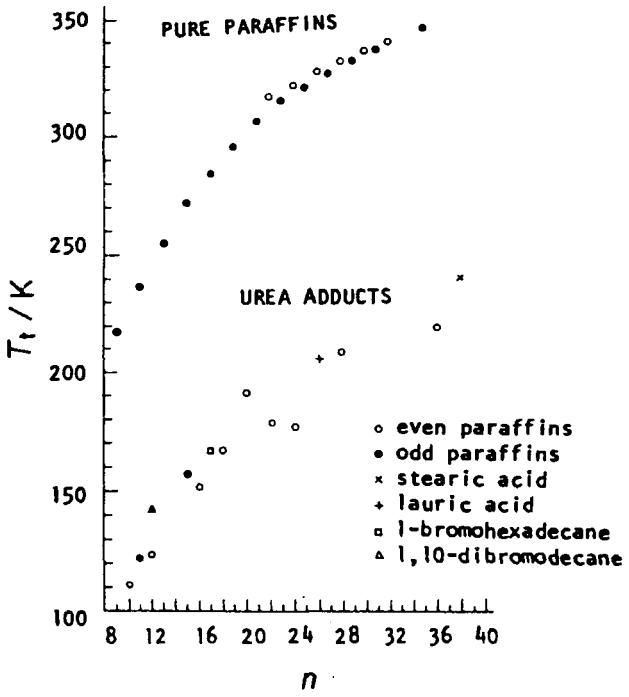

FIGURE 2 Transition temperature against the number of carbon atoms in the guest molecule. Transition temperatures for pure *n*-paraffin crystals are also shown.

if these dimer molecules are regarded as one guest molecule (Figure 2). Similarly Figure 2 shows the transition temperatures of the brominated hydrocarbon adducts regarding the bromine atoms as the terminal carbon atoms of the guest molecules.

The channel length for the sebacic acid molecule, 14.53 A, is about 0.5 A shorter than the length of the fully extended molecule in pure sebacic acid crystals, 15.04 A.[16] From the geometrical viewpoint, sebacic acid molecules linked by O—H···O hydrogen bonds to form an infinite chain structure as in the sebacic acid crystal have to twist appreciably in order to enable them to occupy the urea channel with a hollow of 5 A diameter. The shortening of the channel length, 0.5 A, likely indicates this feature. Again trans 1,4-polybutadiene chain is not planar zigzag, i.e., it consists of the repetition of trans-skew(+)-trans(double bond)-skew(−) conformations in the urea adduct.[10] Accordingly the shape of the cross-section of the guest molecule about the channel axis seems to affect crucially whether the adduct undergoes the phase transition or not, i.e., a guest molecule possessing cylindrical

cross-section does not allow the deformation of the urea channel irrespective of the magnitude of motion of the guest molecule.

CRYSTAL DATA AND DEFORMATION OF CHANNEL

The crystal data of the high- and low-temperature forms of the n-$C_{16}H_{34}$ adduct are as follows.

High-temperature form: hexagonal, $P6_122$, $a_h = b_h = 8.227 \pm 0.004$ A, $c_h = 11.015 \pm 0.006$ A (298 K).

Low-temperature form: orthorhombic, $P2_12_12_1$, $a_o = 8.263 \pm 0.008$ A, $b_o = 13.871 \pm 0.010$ A, $c_o = 10.988 \pm 0.012$ A (98 K).

Figure 3 shows the a- and b-cell dimensions of the n-$C_{16}H_{34}$ adduct as a function of temperature, where the high-temperature form is expressed as an orthohexagonal crystal with $b = (3)^{1/2}a$. The cell dimensions change drastically at the transition temperature and anisotropic thermal expansion of the lattice occurs in the low-temperature form; the thermal expansion along the a-axis is negative indeed in the observed temperature range. When the linear thermal expansions in both crystalline forms are expressed conventionally as

$$a = a_0[1 + \alpha_a(T - 273.15\ \text{K})] \quad \text{and} \quad b = b_0[1 + \alpha_b(T - 273.15\ \text{K})],$$

the constants a_0, b_0, α_a and α_b are as follows.

High-temperature form:

$$a_0 = 8.214 \pm 0.004\ \text{A}, \qquad \alpha_a = (5.75 \pm 0.36) \times 10^{-5}\ \text{K}^{-1}$$

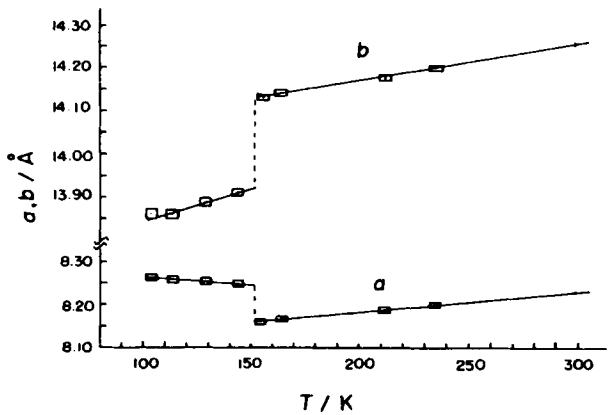

FIGURE 3 The a- and b-unit cell dimensions as a function of temperature for the n-$C_{16}H_{34}$-urea adduct.

Low-temperature form:

$$a_0 = 8.178 \pm 0.008 \text{ A}, \qquad \alpha_a = (-6.08 \pm 0.20) \times 10^{-5} \text{ K}^{-1}$$

$$b_0 = 14.091 \pm 0.011 \text{ A}, \qquad \alpha_b = (9.96 \pm 0.13) \times 10^{-5} \text{ K}^{-1}$$

All other adducts which undergo the phase transition behaved quite similarly as exhibited by the n-$C_{16}H_{34}$ adduct. For example, for the $CH_3(CH_2)_{15}Br$ adduct, $\alpha_a = 5.02 \times 10^{-5}$ K^{-1} for the high-temperature form and $\alpha_a = -5.67 \times 10^{-5}$ K^{-1} and $\alpha_b = 7.33 \times 10^{-5}$ K^{-1} for the low-temperature form. Such a remarkable anisotropic thermal expansion in the low-temperature form is an indication of the enhancement of the deformation of the urea channels with lowering temperature and it should be closely related to the temperature dependence of the oscillational motion of the guest molecules about the channel axis. The thermal expansion along the c-axis has not been obtained. However, the c-dimension at 153 K, just above the transition temperature of the n-$C_{16}H_{34}$ adduct, was 11.007 A, and a drastic change in the c-dimension at the phase transition temperature has not been recognized within the experimental accuracy.

ORIENTATION OF GUEST MOLECULE

Figure 4 shows the electron density distributions viewed along the channel axis for the two crystalline forms of the n-$C_{16}H_{34}$ adduct. In the low-temperature form the guest molecules are orderly disposed and the deformation of the urea channel is also involved. However, the scheme of hydrogen bondings among the urea molecules is retained, except a small distortion, through the phase transition. The hydrogen bonding pattern in such deformed urea channels was reported for the 1,3-butadiene-urea adduct.[10]

In the high-temperature form, on the other hand, the guest molecules are oriented statistically with six-fold rotation symmetry on this projection. Smith[2] reported, in his X-ray study of the high-temperature form of the n-$C_{16}H_{34}$ adduct, that two statistical models possessing two distinct orientations of the guest molecules and a free rotator model gave small differences in the structure factors. He adopted, however, a statistical model in which the molecular plane of a guest molecule is perpendicular to the (100) plane (Figure 10 in Ref. 2). Hereafter orientation of the molecular plane is denoted in terms of the "setting angle χ", where $\chi = 0°$ is defined as the molecular plane parallel to the ac-plane in both crystalline forms (Figure 1). Therefore, the setting angle in the high-temperature form proposed by Smith is $\chi = 30°$.

The contributions of the guest molecules to the $hk0$ structure factors were considered for three extreme cases, i.e., two statistical models with setting

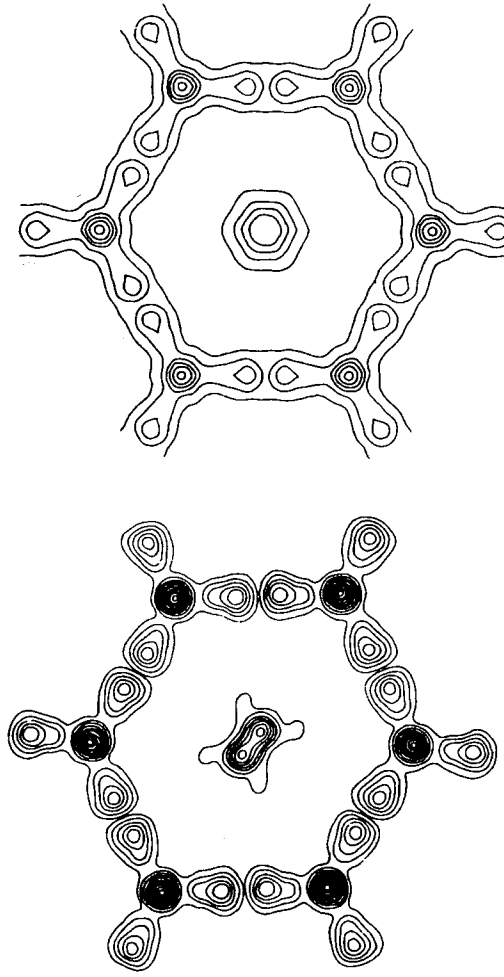

FIGURE 4 Electron density projections along the channel axis for the n-$C_{16}H_{34}$-urea adduct. (top) High-temperature form. (bottom) Low-temperature form. Intervals of contour lines are 2 e · A^{-2} starting at 4 e · A^{-2}. Dotted lines are 2 e · A^{-2}.

angle of $\chi = 0°$ and 30°, respectively, and the free rotator model. Using the series of Bessel functions, as in the case of helical polymer chains,[17] the structure factor for the guest molecules is expressed as follows.

$$F(kh0) = \sum_n \sum_j f_j J_n(2\pi R r_j)\exp[in(\psi - \phi_j) + \pi/2]$$

where coordinates of the atoms and reciprocal space are expressed by polar coordinates (r, ϕ) and (R, ψ), respectively, f is the atomic scattering

factor, $r_C = 0.44$ A, $r_H = 1.425$ A and ϕ_C is now equal to the setting angle χ. Within the limiting sphere in the reciprocal space observed with copper Kα radiation, the orders of Bessel functions which should be taken into account are $n = 0$ and ± 6 for the two statistical models and only $n = 0$ for the free rotator model.

The difference in $F(hk0)$ between the two statistical models is then

$$\Delta F_1 = F_{\chi=0^\circ} - F_{\chi=30^\circ} = -32[f_C J_6(2\pi R r_C)\cos \Psi + 2f_H J_6(2\pi R r_H)\cos 6\psi \cos 6\phi_H]$$

Using the geometrical condition, $\phi_H = 40^\circ$,

$$\Delta F_1 = -32[f_C J_6(2\pi R r_C) - f_H J_6(2\pi R r_H)]\cos 6\psi.$$

Similarly the difference between the free rotator model and the two statistical models are

$$\Delta F_2 = \mp \frac{\Delta F_1}{2},$$

where upper and lower signs are for the models of $\chi = 0^\circ$ and 30°, respectively. Figure 5 shows ΔF_1 as a function of R, and indicates that ΔF_1 is sensitive only in the range between $R = 0.3$ and 0.9 A^{-1}. In this range, agreement between the observed and calculated structure factors seems slightly better for the model $\chi = 0^\circ$ than for the model $\chi = 30^\circ$. It is, however, difficult to conclude from this result alone that the model $\chi = 0^\circ$ is better than the free rotator model. Fortunately, the signs of $F(hk0)$'s for the three models are the same for all observed reflections. Therefore two $F_o - F_c$ syntheses were undertaken, where F_c included only non-hydrogen atoms for the models $\chi = 0^\circ$ and 30°, respectively. The syntheses showed essentially the same peaks of hydrogen

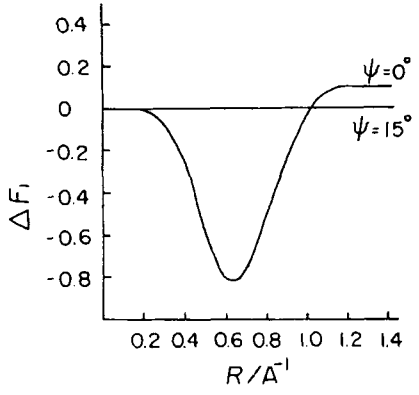

FIGURE 5 ΔF_1 vs. R. The thermal parameter is assumed to be 6.0 A^2.

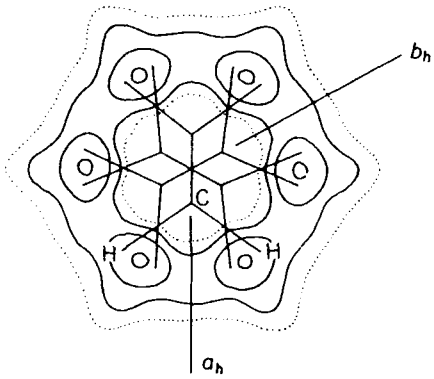

FIGURE 6 $F_o - F_c$ synthesis for ($hk0$) of the high-temperature form of the n-$C_{16}H_{34}$-urea adduct. Intervals of the contour lines are 0.5 e · A^{-2} starting at 0 e · A^{-2} which are shown by dotted lines.

atoms of guest molecules which are well interpreted by the statistical model $\chi = 0°$ (Figure 6).

Potential energy calculation, in which the 6–12 Lennard-Jones type van der Waals interaction energy between urea molecules and the n-$C_{16}H_{34}$ molecule was taken into account, was carried out varying the setting angle χ and the z-coordinate of the guest molecule along the channel axis (c-axis). The atomic coordinates of urea molecules were taken from the X-ray results at 298 K by Smith and at 153 K and 98 K by us; the paraffin chain was assumed to be planar zigzag. The potential energy calculation indicated that, whenever three different parameter sets of the potential function, the sets I and II by Parsonage and Pemberton[18] and the set by Go and Scheraga[19] were used, the potential maxima and minima appeared at the same setting angles irrespective of the z-coordinate. There are four minima for the low-temperature form and six minima for the high-temperature form in the energy maps, E vs. χ. Examples of the energy maps are shown in Figure 7.

The lowest potential minima for the low-temperature form are about $\chi = -30°$ and 150° at 98 K. The setting angles obtained from the energy calculation are then fairly accordance with the X-ray result, $\chi = -32.6°$ and 147.4°.

On the other hand, the energy calculation for the high-temperature form strongly suggests that the setting angles are approximately 0° and multiples of 60°, i.e., $\chi = 0°$. The energy calculation together with the X-ray analysis thus supports that the equilibrium setting angle alters about 30° through the phase transition (Figure 1).

In the low-temperature form, an overall molecular rotation jumping from one site to another site is forbidden by the high potential barriers, about

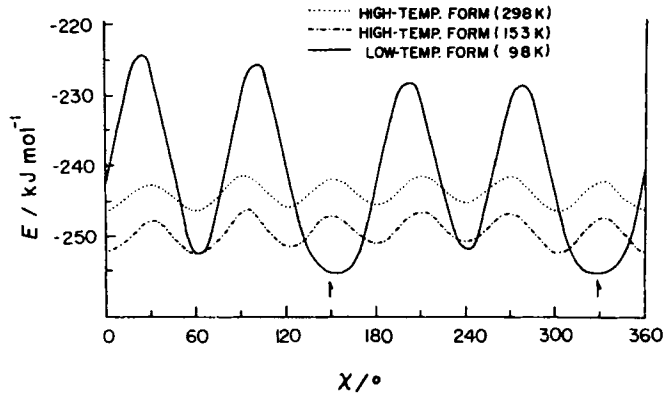

FIGURE 7 Potential energy curves against the rotation of guest molecule for the n-$C_{16}H_{34}$-urea adduct. Arrows indicate the setting angles obtained from X-ray analysis. Set II of Parsonage and Pemberton was used as the parameters of potential function.

30 kJ mol^{-1}. However, the wells at the potential minima are rather wide. Therefore an appreciable rotational oscillation of the guest molecule would be feasible. Gilson and McDowell[3] and later Umemoto and Danyluk[4] studied the broad-line NMR of several urea-d_4 adducts with n-paraffins. According to these studies, the guest molecules are not rigid at 95 K: the methyl groups are rotating freely on the NMR scale, and a partial rotational oscillation of the guest molecules is also invoked, in particular for short chain paraffins. Umemoto and Danyluk also indicated that the marked line-narrowing transition temperatures correspond roughly to the transition temperatures obtained by the heat capacity measurement.[1,2] The temperature range of line-narrowing transition for the stearic acid-urea-d_4 adduct, 220 to 230 K as estimated from Figure 6 in Ref. 4, again seems to be corresponded to the transition temperature of 239 K obtained in the present DTA measurement. Connor and Blears[6] also detected distinct minima in T_1 and $T_{1\rho}$ curves at 231 K for the stearic acid adduct.

The correspondance of the transition temperatures obtained by NMR and thermal measurement was confirmed for the n-$C_{20}H_{42}$-urea-d_4 and $Br(CH_2)_{10}Br$-urea-d_4 adducts as shown in Figure 8. The second moment of the n-$C_{20}H_{42}$ adduct decreases gradually over a wide temperature range as compared with the $Br(CH_2)_{10}Br$ adduct and several adducts reported previously.[3,4] This reason is still uncertain but the thermal measurement of the n-$C_{20}H_{42}$ adduct by Pemberton and Parsonage[1,2] and also by us showed a wide temperature range of transition.

The general features of the NMR spectra appear to be well interpreted from the present structural aspect. In the low-temperature form, the wide

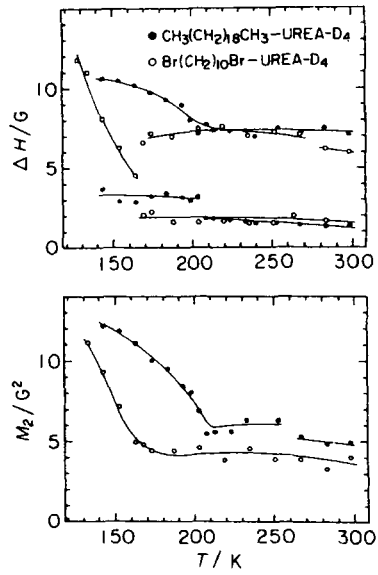

FIGURE 8 Line-widths and second moments for the $Br(CH_2)_{10}Br$-urea-d_4 and n-$C_{20}H_{42}$-urea-d_4 adducts.

wells at the potential minima seem to allow an appreciable rotational oscillation of the guest molecules. Above the phase transition temperature, the hexagonal hollow of the urea channel allows an overall rotation of the guest molecule jumping from one site to the neighboring sites, probably, together with an increment of internal twisting motions, and then the drastic line-narrowing takes place around the phase transition temperature.

It may be inferred from the present study that the general feature of the phase transitions found for many urea adducts with *n*-paraffins and paraffin-type compounds is revealed, although an examination of the details of the correlation between neighboring guest molecules in the channel and the motions of the urea molecules in the high-temperature form is not yet available. Finally, it should be noted that the urea adducts with several ketones which have been used exclusively for the dielectric studies[7–9] exhibited different behaviors in thermal measurement and also X-ray diffraction. Therefore, it is still uncertain whether the informations obtained in this study are applicable to the ketone adducts.

Acknowledgment

The authors wish to acknowledge the interest and support of Professor H. Tadokoro of Osaka University. The authors also wish to thank Chihara Laboratory of Osaka University for the DTA measurement and Mitsui Petroleum Chemical Co. for the NMR measurement.

References

1. Y. Chatani, Y. Taki, and H. Tadokoro, *Acta Crystallogr.*, **B33**, 309 (1977).
2. A. E. Smith, *Acta Crystallogr.*, **5**, 224 (1952).
3. D. F. R. Gilson and C. A. McDowell, *Mol. Phys.*, **4**, 125 (1961).
4. K. Umemoto and S. S. Danyluk, *J. Phys. Chem.*, **71**, 3757 (1967).
5. J. D. Bell and R. E. Richards, *Trans. Faraday Soc.*, **65**, 2529 (1969).
6. T. M. Connor and D. J. Blears, *Mol. Phys.*, **17**, 435 (1969).
7. R. J. Meakins, *Trans. Faraday Soc.*, **51**, 953 (1955).
8. J. I. Lauritzen, *J. Chem. Phys.*, **28**, 118 (1958).
9. P. Dansas, P. Sixou, and M. M. Jaffrain, *Mol. Phys.*, **21**, 225 (1971).
10. Y. Chatani and S. Kuwata, *Macromolecules*, **8**, 12 (1975).
11. M. E. Straumanis, *J. Appl. Phys.*, **20**, 726 (1949).
12. R. C. Pemberton and N. G. Parsonage, *Trans. Faraday Soc.*, **61**, 2112 (1965).
13. R. C. Pemberton and N. G. Parsonage, *Trans. Faraday Soc.*, **62**, 553 (1966).
14. M. G. Broadhurst, *J. Res. Nat. Bur. Stand. A*, **66**, 241 (1962).
15. F. Laves, N. Nicolaides, and K. C. Peng, *Zeit. Krist.*, **121**, 258 (1965).
16. J. Housty and M. Hospital, *Acta Crystallogr.*, **20**, 325 (1966).
17. W. Cochran, F. H. Crick, and V. Vand, *Acta Crystallogr.*, **5**, 581 (1952).
18. N. G. Parsonage and R. C. Pemberton, *Trans. Faraday Soc.*, **63**, 311 (1967).
19. N. Go and H. A. Scheraga, *Macromolecules*, **6**, 525 (1973).